



Analysis of Cavity Conditions in Heavy Ion Beam Fusion Reactors

R.R. Peterson

February 1987

UWFDM-719

***FUSION TECHNOLOGY INSTITUTE
UNIVERSITY OF WISCONSIN
MADISON WISCONSIN***

DISCLAIMER

This report was prepared as an account of work sponsored by an agency of the United States Government. Neither the United States Government, nor any agency thereof, nor any of their employees, makes any warranty, express or implied, or assumes any legal liability or responsibility for the accuracy, completeness, or usefulness of any information, apparatus, product, or process disclosed, or represents that its use would not infringe privately owned rights. Reference herein to any specific commercial product, process, or service by trade name, trademark, manufacturer, or otherwise, does not necessarily constitute or imply its endorsement, recommendation, or favoring by the United States Government or any agency thereof. The views and opinions of authors expressed herein do not necessarily state or reflect those of the United States Government or any agency thereof.

Analysis of Cavity Conditions in Heavy Ion Beam Fusion Reactors

R.R. Peterson

Fusion Technology Institute
University of Wisconsin
1500 Engineering Drive
Madison, WI 53706

<http://fti.neep.wisc.edu>

February 1987

UWFDM-719

ANALYSIS OF CAVITY CONDITIONS IN HEAVY ION BEAM FUSION REACTORS

R.R. Peterson

Fusion Technology Institute
1500 Johnson Drive
University of Wisconsin-Madison
Madison, Wisconsin 53706

February 1987

(Revised September 1987)

UWFD-719

To be published in Fusion Technology.

ANALYSIS OF CAVITY GAS CONDITIONS IN HEAVY ION BEAM FUSION REACTORS

ROBERT R. PETERSON, Fusion Technology Institute, 1500 Johnson Drive,
University of Wisconsin-Madison, Madison, Wisconsin 53706-1687

ABSTRACT

The limits on the cavity gas density required for beam propagation and condensation times for material vaporized by target explosions can determine the maximum repetition rate of Heavy Ion Fusion (HIF) driven fusion reactors. If the ions are ballistically focused onto the target, the cavity gas must have a density below roughly $3 \times 10^{12} \text{ cm}^{-3}$ at the time of propagation; other propagation schemes may allow densities as high as 1 torr or more. In some reactor designs, several kilograms of material may be vaporized off of the target chamber walls by the target generated x-rays, raising the average density in the cavity to $3 \times 10^{18} \text{ cm}^{-3}$ or more. A one-dimensional combined radiation hydrodynamics and vaporization and condensation computer code has been used to simulate the vaporization and condensation of material in the target chambers of HIF fusion reactors. Repetition rates in excess of 1 Hz have been found to be possible in the three types of target chambers studied. Means of increasing allowable repetition rates are discussed.

I. INTRODUCTION

The vaporization and recondensation of material in the reaction chamber of an Inertial Confinement Fusion (ICF) facility can have far reaching consequences on the facility design. If one is designing a plant that produces commercial electrical power, the condensation of vaporized material must be considered because it may put an upper limit on the rate at which targets may be exploded and may have a strong effect on the economic viability of the plant. Both in power plants and in near term devices, where target explosions may be very infrequent, one must consider the effects of condensation on things such as optical components, whose performance or survival may be compromised by the deposition of a layer of material through condensation. There may be beneficial aspects of the recondensation as well, such as redeposition of vaporized material back onto the first wall of the reaction chamber. The complexities of these issues may be avoided by designing facilities that have low target yields and large chamber radii and thus have no vaporization of wall material, but this increases the costs and/or lowers target gain and fusion power. For these and other reasons, understanding the vaporization and condensation of material in reaction chambers is a critical part of technology research for ICF.

The economic feasibility of heavy ion beam driven fusion reactors as power plants depends on the ability to achieve a high rate of target shots. This may be even more true for Heavy Ion Fusion (HIF) than it is for laser or light ion beam driven fusion because of characteristics of HIF drivers; HIF drivers have traditionally been thought to have the potential for high repetition rates. Two recent studies have found that the cost of electricity for HIF power plants decreases sharply with increasing repetition rate for

repetition rates below 4 Hz.^{1,2} The required shot rate depends on the cost of the plant, the desired cost of electricity, and the target gain. A high total repetition rate for the plant can occur through a high rate for each target chamber, multiple target chambers, or a combination of the two. The allowable repetition rate for various target chamber designs is the topic of this paper.

There are several types of designs for target chambers for HIF reactors. The repetition rate for a given target chamber is determined by the required cavity gas conditions at the time of the next shot and the length of time needed to achieve these conditions. If there is no material vaporized off of the chamber walls, which is the case in designs where the target energy density on the walls is low,³⁻⁵ very high repetition rates may be possible. Another approach is to allow a thin sacrificial layer from the first wall of the cavity to be vaporized and recondensed back onto the wall.⁶⁻⁸ The advantage of this is that the cavities can be smaller and cheaper, or so the designers hope. Also, one could use higher gain targets that might improve the economy of power production. Here, one would need a driver with more energy per pulse and one would therefore have to consider the effect of the increased driver costs on plant economics. On the other hand, one must wait until the vapor density in the cavity has fallen to the point where beam propagation is possible before firing the next shot and there is the chance that the vapor could condense on and damage critical components of the reactor.

The vaporization of first wall material and its condensation back onto the walls can be a very complicated process.⁹ The target generated x-rays rapidly vaporize the wall material in an as yet poorly understood way. For example, the x-rays raise some of the wall material that is not on the surface

to an energy density above that required to heat it to the boiling point but not enough to overcome the latent heat of vaporization and it is unclear what happens to this material. The vaporized material forms a dense layer of plasma near the surface, which is heated by target generated ions, that may exist long enough for some rather unusual chemistry to take place.¹⁰ The initially very nonuniform pressure profile in the vapor causes a shock wave moving towards the center of the target chamber that eventually collides with other similar shocks, resulting in very complicated hydrodynamic motion on the target chamber gases and vapors. While this motion is occurring, the gas is radiating energy back to the first walls and is condensing. Both of these processes put significant surface heat fluxes onto the wall that can cause evaporation of wall material. Unusual molecular species formed shortly after the vaporization may have a rather low sticking coefficient or may actually cause the wall to release more material than is condensed. Eventually, the vapor cools enough and enough energy has been conducted away through the walls that condensation proceeds to the point that the ion beam can be propagated through the gas and the next shot is fired. The complex nature of these phenomena indicates that a well tested computer code that contains simulations of the relevant physical processes is required as a design tool.

In this paper, I will present calculations of the time-dependent average gas density in a target chamber. I will do this for three target chamber designs that allow the first wall to partially vaporize: HIBALL,⁶ the wetted wall concept,⁷ and CASCADE.⁸ I will begin with a comparison of the target chamber gas densities allowed by different drivers and propagation schemes. I will then discuss the physics that goes into the computer code used for these calculations. Following a short discussion of HIF target spectra, I will then

present the results of the calculations for the three designs and will consider what can be done to improve the repetition rates for the designs.

II. GAS CONDITIONS REQUIRED FOR HEAVY ION BEAM PROPAGATION

The limitation of the reaction chamber repetition rate by vaporization and recombination may be a very important consideration for ICF power plants. This limit comes about because the density of the gas in the chamber at the time of the next shot is determined by the mode of propagation for the driver beam. Lasers require a density of between $3 \times 10^{13} \text{ cm}^{-3}$ and $3 \times 10^{16} \text{ cm}^{-3}$, light ion beams $3 \times 10^{16} \text{ cm}^{-3}$ to more than $3 \times 10^{18} \text{ cm}^{-3}$, and heavy ion beams $3 \times 10^{12} \text{ cm}^{-3}$ to $3 \times 10^{17} \text{ cm}^{-3}$ depending on the mode of propagation. There is considerable uncertainty in these limits.

The breakdown of gases with intense laser beams has been extensively studied theoretically and experimentally.^{11,12} Calculations of the breakdown threshold laser intensities within the multiphoton absorption and cascade models do not always agree with experimental results, which are themselves somewhat inconsistent. It has been found that the breakdown threshold depends greatly on the laser pulse width and frequency, the focusing optics,¹³ and the gas involved, including the density, specie and impurities. An additional complication is that if the breakdown is limited to a small part of the beam path, much of the laser energy may still reach the target, especially if the breakdown occurs very near to the target as it is likely to do.¹⁴ This all means that it is very difficult to state generally the density limits on the reaction chamber gas, because it is strongly dependent on the design of the facility.

The gas density limits in the case of light ion beam fusion depend on the mode of beam propagation. Propagation in laser guided plasma channels is currently the favored scheme.¹⁵⁻¹⁸ For correct channel formation the gas mass density in the target chamber should be about $2 \times 10^{-5} \text{ g/cm}^3$. The species of the gas ranges from hydrogen to xenon, but is always a noncondensable gas. The number density ranges from $6 \times 10^{16} \text{ cm}^{-3}$ for xenon to $1 \times 10^{19} \text{ cm}^{-3}$ for hydrogen. The effects of condensable vapor mixed in with background gas may be significant to the formation of the channel and the behavior of the fireball in the gas that results from the target explosion,¹⁹ but numerical limits on the condensable density are not known. In the past, we have used the condition on the condensable vapor density that it cannot change the total mass density by more than 10%. As an alternative to propagation in channels, schemes using co-moving electron beams²⁰ to charge and current neutralize the ion beam have also been considered. These methods typically require cavity gas densities on the order of $3 \times 10^{12} \text{ cm}^{-3}$.

Heavy ion fusion has several beam propagation schemes, with required target chamber gas densities ranging from $3 \times 10^{12} \text{ cm}^{-3}$ to roughly 10^{18} cm^{-3} .²¹ The lowest target chamber gas densities are required by ballistic focusing of heavy ion beams. As one increases the cavity gas density, there is increased ion loss due to scattering. As the density continues to increase, the background gas provides some charge and current neutralization. However, at low gas densities there exist two-stream instabilities in the background plasma-ion beam system that prevent effective ion beam propagation. Once the density reaches a level of about $3 \times 10^{15} \text{ cm}^{-3}$,²² the collision frequency in the plasma becomes high enough to damp out the plasma instabilities to the point that the ion beam may propagate in a charge and

current neutralized mode. At higher densities, plasma channels could possibly be used in much the same way as in light ion fusion. Other means of beam propagation include propagation in a self-pinched mode, which is possible at a somewhat lower density.

From the discussion above, one can see that the vapor density required at the time of beam propagation can vary over about six orders of magnitude depending on the mode of propagation. Any material that is vaporized by the target explosion must condense at a sufficient rate that the density reaches the required level before the next shot. The calculation of the amount of vaporization of first wall material and of that rate of condensation is the topic of the remainder of this paper.

III. COMPUTER MODELING OF THE PHYSICS OF VAPORIZATION AND CONDENSATION

The vaporization and recondensation of material in the target chamber of an ICF reactor are often broken down into two distinct phases.²³⁻²⁵ The vaporization can be of two types: rapid adiabatic vaporization that is due to essentially instantaneous absorption of target generated x-rays and slow vaporization due to energy that is radiated from the target chamber gas over a longer enough time that vaporization is limited by heat transfer into the material. In a reactor with a low cavity gas density, which I will call case 1, the x-rays from the target deposit mostly in the first surface that they meet in the target chamber, whereas in reactor schemes with higher gas densities, hereafter referred to as case 2, this energy is mainly absorbed in the gas. In case 1 both superheated vapor and vapor at the local boiling temperature of the vaporizing material come off of the surface in a very complicated way. This vapor will then meet with the energetic target debris ions and will be

further heated. Over the next 100 ms or so the vapor will radiate to the first surface, causing additional vaporization, hydrodynamically move throughout the target chamber, and condense back onto the first surface. In this case, the presence of noncondensable gases may or may not affect the rate of condensation. In case 2, the x-ray and debris energy from the target create a fireball in the target chamber gas that radiates its energy to the first surface over a time on the order of 0.1 ms. The radiant energy of the first surface is spread out over a long enough time that heat conduction into the material can drastically reduce the amount of vaporization. The vaporized material then mixes in with the noncondensable target chamber gases, where it is moved about the target chamber by the hydrodynamic motion of the fireball and is eventually condensed back out of the noncondensable gases. The rate of condensation can be greatly reduced by the presence of the noncondensable gases.

In both of the scenarios described above, similar physical phenomena must be considered. In many cases, heat transfer through the first surface material is the major process that determines the condensation rate.²⁶ Slow heat transfer through the material can keep the temperature near the surface high, which causes a high vapor pressure that slows the net condensation rate. In a liquid metal first surface, one must be aware that convective heat transfer can decrease the surface temperature and increase the condensation rate.²⁷ Hydromotion in the target chamber gas can also play a role by affecting the radiative heat transfer and the local vapor density adjacent to the first surface. The physics of the sticking of vapor atoms onto the condensing surface is very complicated,¹⁰ being affected by the molecular state of the vapor, the energy of the condensing atoms, and the state of the

condensing surface. The molecular state of the vapor is determined in case 1 during the time shortly after the rapid vaporization and deposition of debris ions, when the vapor is very hot and dense. In fact, there are other important processes occurring at this time: there may be rapid recondensation because the vaporized mass is still very close to the first surface, there may be additional vaporization because the vapor has been heated by the debris ions so that the heat flux to the surface is very high, or both. In case 1, the physics of vaporization itself is rather complex and great differences in the vaporized mass can be predicted by equally reasonable vaporization models.

A computer code, called CONRAD,²⁸ has been under development at the University of Wisconsin that attempts to model many of these physics issues. With the use of this code, much can be learned about the relative effects of the aforementioned issues. However, it is clear that, both to study each item separately and to benchmark the computer code, experiments are needed. A project is in progress to verify the accuracy of the CONRAD computer code by comparison with that experimental data which is presently available.²⁹ There are presently no experiments that simultaneously simulate all of phenomena that occur in HIF target chambers. However, experiments do exist that can be used to verify various aspects of CONRAD. The coupling of incident ions to the target chamber gas and the hydromotion of the gas can be compared with experiments being done at the Naval Research Laboratory, where laser created blow-off plasmas drive shocks in background gases.³⁰ Experiment at Sandia National Laboratory³¹ and other laboratories,^{32,33} where stress waves in solids that are subjected to intense x-rays are measured, may be able to provide x-ray deposition profiles and amounts of mass vaporized, which can be compared with CONRAD. The equations-of-state and radiation opacities in

CONRAD, which are provided by the code MIXERG,³⁴ are being compared with data from Los Alamos National Laboratory.³⁵

The CONRAD computer code attempts to model the behavior of a radiating, moving vapor and a material that is vaporizing or on which vapor is condensing by dividing the problem into two separate regions. The vapor, one of the regions, is modeled with Lagrangian hydrodynamics and multigroup radiative heat transfer. The unvaporized material, the other region, is modeled with a standard finite difference heat transfer method. From this point on, the term "material" will refer to the unvaporized material. Each of these regions is treated with standard numerical techniques. There is little experience in how to model the heat and mass transfer between the two regions. For this reason, there have been some options written into the code that allow the user to choose, for example, what model to use for rapid vaporization.

There has been considerable effort devoted to modeling the coupling between the target explosion and the vapor and between the material and the vapor. Multigroup x-ray deposition in the gas and surface material is calculated either as though it were instantaneous or in a time-dependent manner, or both ways. The energy from target debris ions is deposited in the gas as calculated by a modified form of Mehlhorn's model.³⁶ The time-of-flight of the ions is considered. The Lagrangian zones are dynamically rezoned as mass is transferred between the surface material and the vapor. Data tables of equations-of-state and opacities are read by CONRAD and are provided by the MIXERG computer code.³⁴

In the past, CONRAD has been used to study the importance of radiative heat transfer from the vapor to the first surface on the net condensation rate.⁶ It was found that energy radiated from the vapor, over a time long

compared to the heat pulse directly from the target and short compared to the thermal diffusion time in the surface material, can cause significant additional vaporization that slows the overall reduction of the vapor density. CONRAD simulations have also shown that the temperature and mass of the condensing particle, by affecting the mobility of the particles and thus their diffusion speeds, can have a marked effect on the condensation rate. The effects of vaporization modeling and vapor density dependent boiling temperatures have been studied.

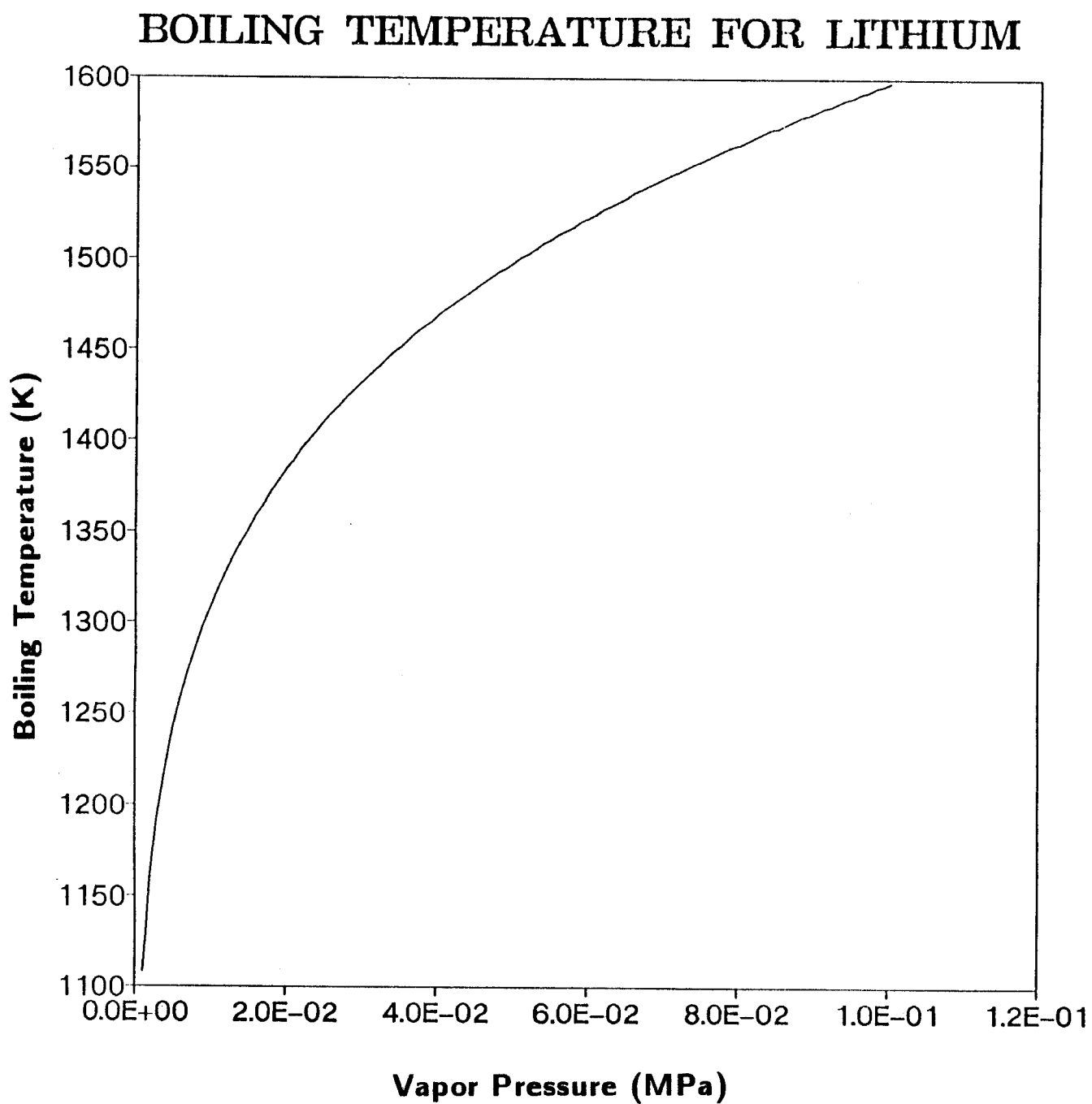
An effect that may seriously limit the condensation rate is that the equilibrium boiling temperature of the condensing material is a function of the local vapor density. Or, in a microscopic sense, the evaporation rate is a function of the surface temperature of the material, while the condensation rate is a function of the properties of the vapor near the wall; the net condensation rate is the difference between the two. The choice of these alternative approaches to the same effect is a option in CONRAD.

The macroscopic equilibrium model uses a temperature dependent calculation of the boiling temperature and then uses the rapid vaporization models to calculate the amount of evaporated mass on each time step. Using the Clausius-Claperyon equation, one can deduce that the boiling temperature at some pressure P is related to the boiling temperature at 1 atmosphere by

$$T_{\text{boiling}} = \frac{1}{\left[\frac{1}{T_{\text{boiling}}(P=1 \text{ atm})} - \frac{R}{\Delta H_v} \ln \left(\frac{P}{1 \text{ atm}} \right) \right]} \quad (1)$$

where P is the local partial pressure of the vapor in atmospheres, R is the gas constant and ΔH_v is the latent heat of vaporization. In Fig. 1, the boiling temperature of lithium is plotted against the vapor pressure. We are

Fig. 1. Lithium Boiling Temperature Versus Local Vapor Pressure.



aware that the latent heat of vaporization is not always approximately constant and that experimental data are available for some materials over a range of temperatures. The use of equation 1, however, lets us investigate materials such as $\text{Pb}_{83}\text{Li}_{17}$ for which experimental data over the complete range of interest are not yet available.

The microscopic evaporation model just assumes that those ions on the surface of the material that have enough thermal speed to overcome the escape potential of the surface will leave the surface. The atoms on the surface have a distribution of speeds that are a function of the surface temperature that lead to an equation for the evaporation rate,

$$\dot{m} = \rho \sqrt{\frac{T_{\text{surf}} 4.13 \times 10^3}{A}} \exp\left(-\frac{121 \Delta H_v A}{T_{\text{surf}} \rho}\right) . \quad (2)$$

Here ρ is the mass density of the surface material, T_{surf} is the surface temperature in K and A is the atomic mass number of the material.

We have compared the use of the two condensation options. The macroscopic model assumes that the system is in a quasi-steady-state, where the condensation rate approximately equals the vaporization rate. However, in HIF target chambers the surface temperature and the gas density can be changing rapidly, which can lead to situations that are not in a quasi-steady-state. We have found that CONRAD predicted unphysical behavior in these situations. The microscopic approach does not require quasi-steady-state because the condensation and evaporation rates are calculated independently. We have tested the microscopic method by running CONRAD simulations to long times to insure that the gas pressures approach the steady-state vapor

pressures. Therefore, we have used the microscopic method for calculating net condensation rates in all of the following results.

IV. HEAVY ION FUSION TARGET EXPLOSIONS

The x-ray and ion spectra and energy partitioning that result from the target explosion are required for analysis of the target chamber behavior. We have chosen the target designed by Bangerter, et al. as one that is typical for HIF.³⁷ Work has continued in recent years on this type of HIF target that has lead to new gain-energy curves, but the target design has remained about the same.³⁸ This target design was slightly modified into the form shown in Fig. 2. Here the target is shown in its initial form and in its configuration at the start of its burn. The burning of the target was simulated with the PHD-IV computer code.³⁹

This simulation, in concert with calculations of the interaction between the fusion neutrons with the fully compressed target, provides the time-dependent spectrum of x-rays leaving the target and the debris ion energies. These results have been reported elsewhere,^{40,41} and are also shown in Fig. 3 and Table I. The target yield in these results is normalized to 100 MJ, where the input ion beam energy was 1.3 MJ. The x-ray spectrum shown is integrated out to 3.5 ns, where the hard component is due to x-rays from the burning fuel, while the soft are from the whole target.

Naturally, different reactor designs demand different target yields. These are obtained by scaling the results for 100 MJ to the proper yield. The shapes of the x-ray and ion spectra remain the same, but the numbers of photons and ions are changed.

Table I. HIF Target Yield Energy Partition and Ion Energies

Energy Partition

Fusion Yield	100 MJ
Neutron Yield	71 MJ
X-Ray Yield	20 MJ
Debris Ion Yield	7.4 MJ
Endoergic Neutron Reactions	1.6 MJ

Debris Ion Energies

Debris Ion Yield	7.4 MJ
Average Energy per Nucleon	0.85 keV/amu
Deuterium	1.70 keV
Tritium	2.55 keV
Helium	3.40 keV
Lithium	5.90 keV
Lead	176 keV

Fig. 2. Heavy Ion Fusion Target.

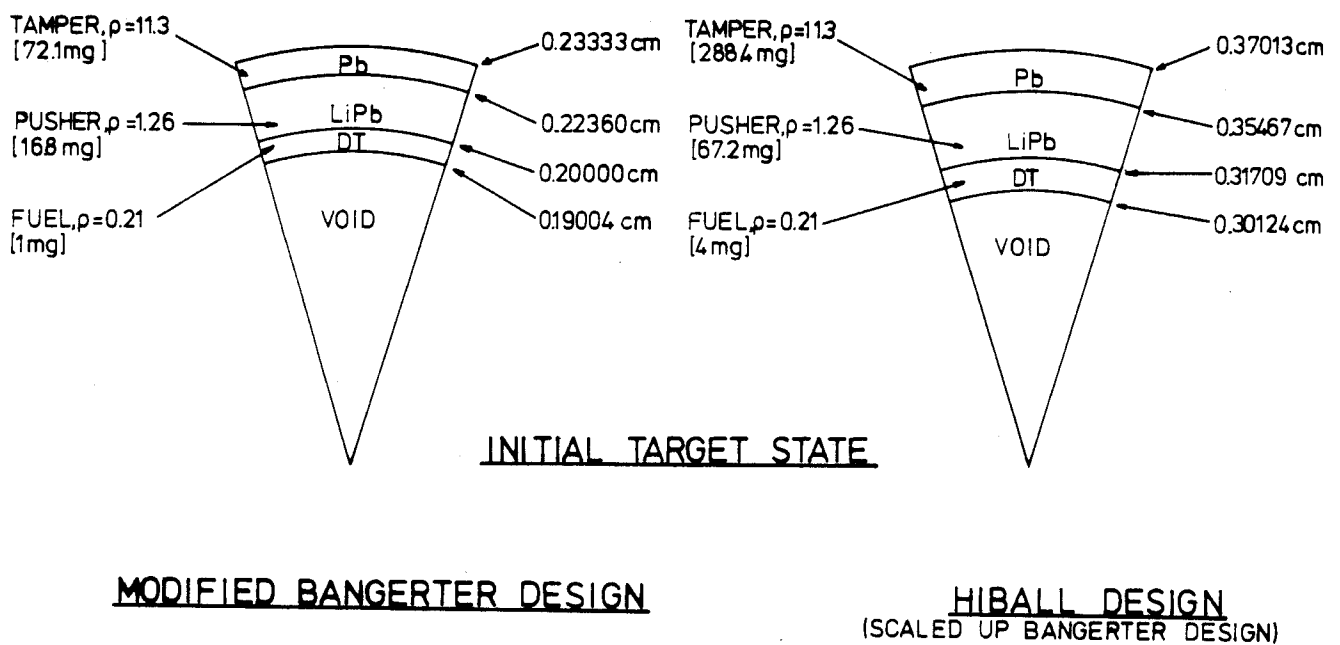
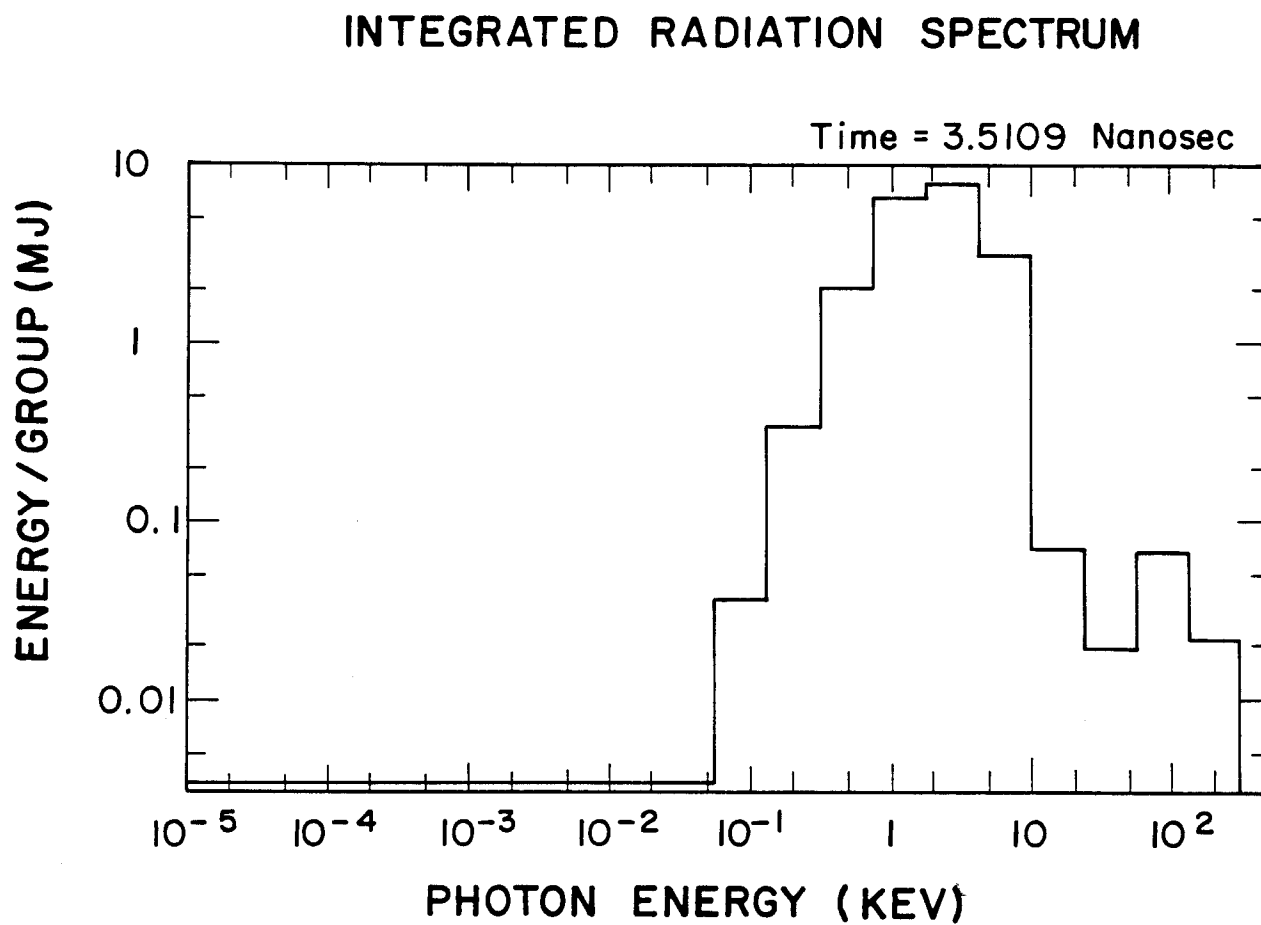


Fig. 3. Target X-ray Spectrum.



V. VAPORIZATION OF FIRST WALL MATERIAL

The vaporization and condensation of lithium in an ICF target chamber have been simulated with the CONRAD computer code. The initial conditions for this simulation are listed in Table II. These parameters are consistent with the Los Alamos National Laboratory wetted-wall concept,⁷ which was chosen for the sake of an example, but do not necessarily represent a design currently under consideration. The x-ray spectrum used for a 30 MJ target explosion is scaled from Fig. 3 and the deposition power profile it instantaneously creates in liquid lithium is given in Fig. 4. The long tail is due to the hard component of the x-rays. The energy of the debris ions has been put into the lowest energy x-ray bin for these calculations. This will have some effect on the results and will not do the heating of the vapor by ions properly. However, since the ions typically take 10^{-6} seconds to deposit their energy, and since the ion deposition lengths are short compared to the x-ray deposition lengths, the ions stop in material already vaporized by the x-rays and will not affect the vaporization process much. A new ion stopping package is currently being tested and better simulations will be done.

Three vaporization models are included in CONRAD, the user's choice of model being an input parameter. The models can be understood with the help of Fig. 5. Here the energy density after deposition of x-rays in the surface material is plotted against distance from the surface nearest the target, as is the energy density needed to raise the material to the boiling temperature and that needed to vaporize the material. One should notice that in region I there is more than enough energy present to vaporize the material and that in region II there is more than the sensible heat required to raise the material to the boiling point but not enough to vaporize it. There is a third region

Table II. Conditions for Computer Simulation

First Surface	Liquid lithium
Nominal Target Yield	25 MJ
First Surface Position	2 meters from target
Target X-Ray Spectrum	Bangerter et al.
Time Dependence of X-Ray Pulse	Instantaneous
Desired Repetition Rate	10 Hz

Fig. 4. Deposition Power in Lithium for Spectrum in Fig. 3. Distance from target is 2 meters.

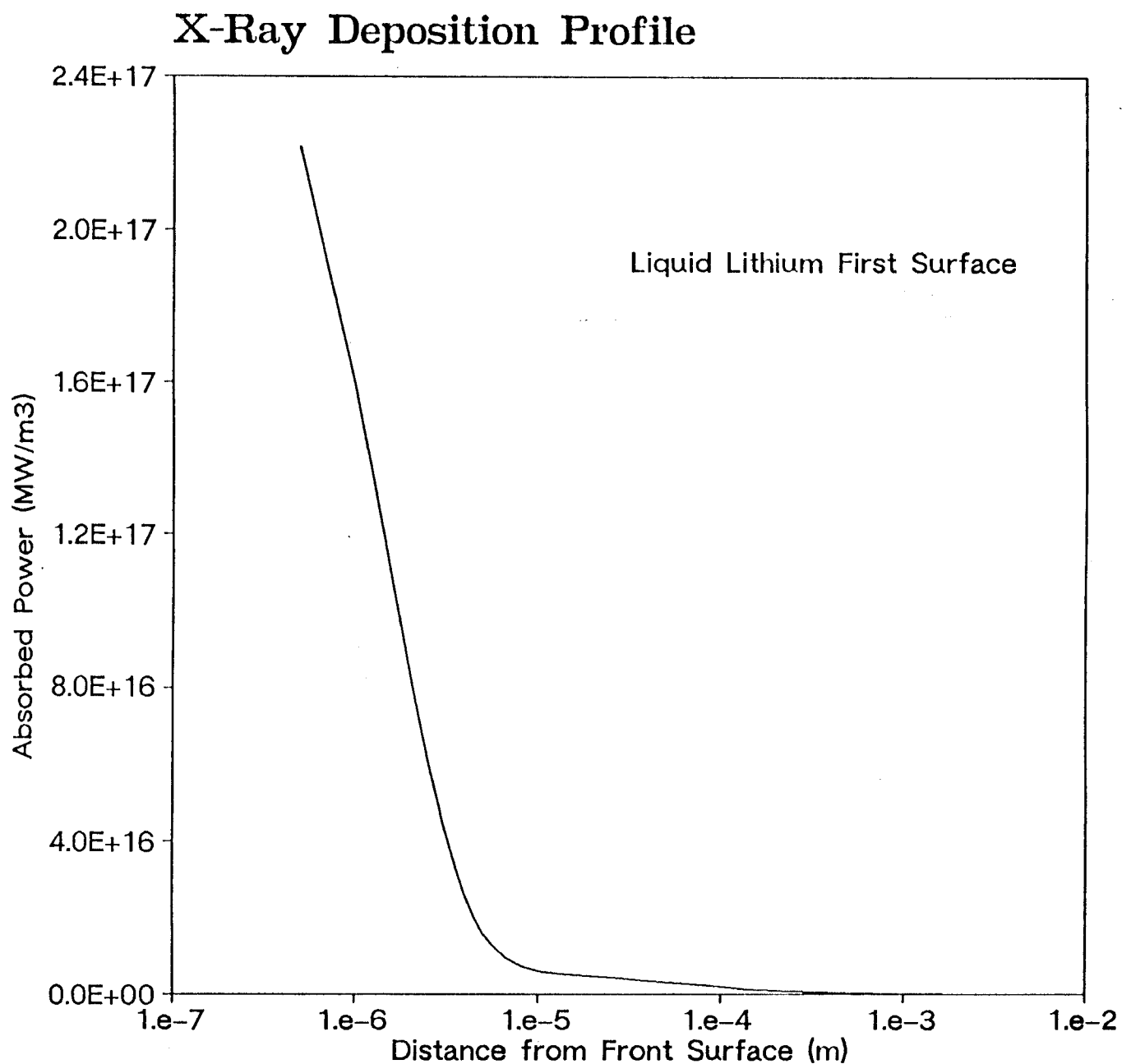
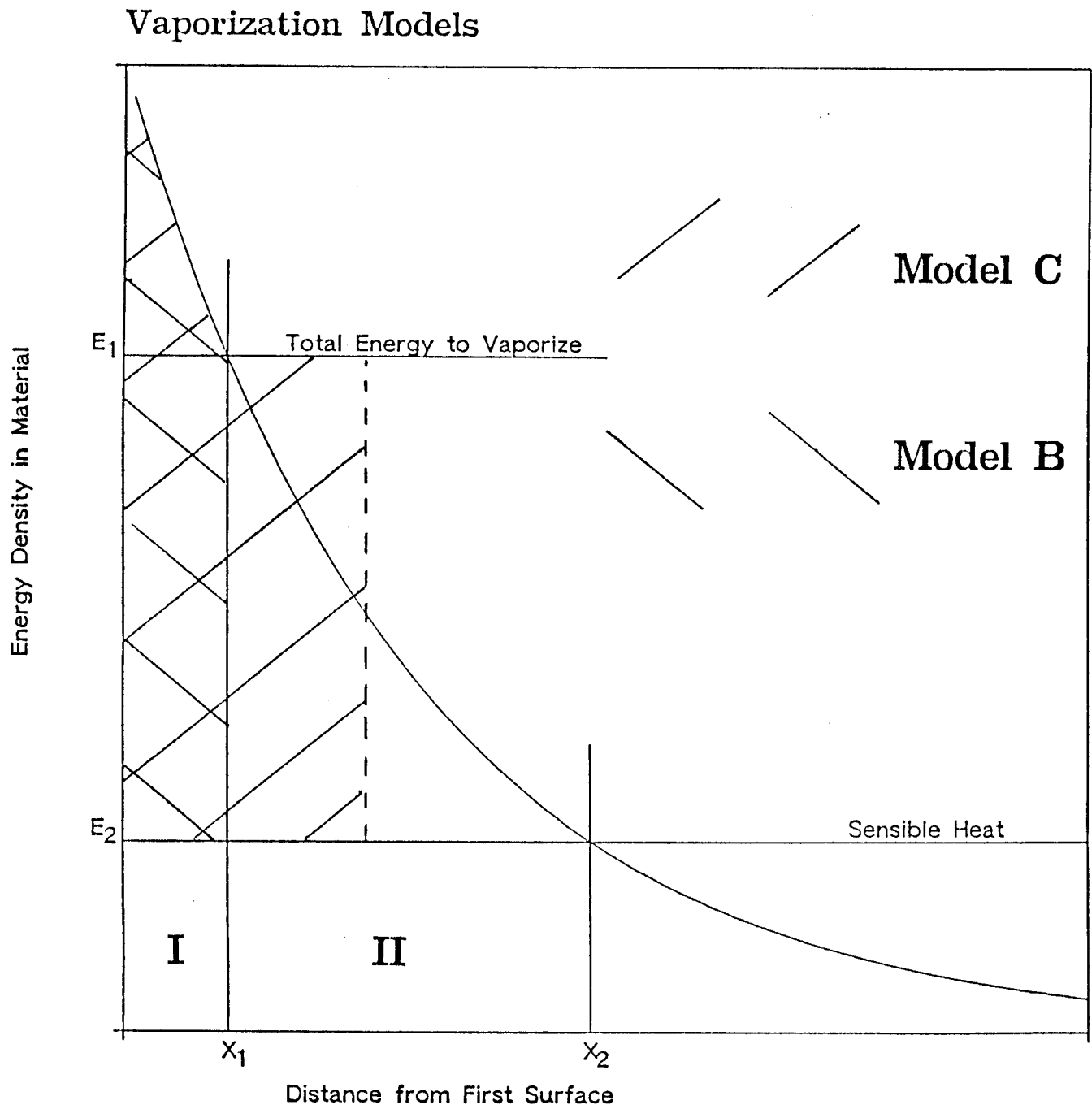


Fig. 5. Vaporization Models.



where the material is below the boiling point. Three different models have been used to study this situation: model A, which is not shown in Fig. 5, assumes that all of the energy from regions I and II is free to spread around to vaporize the maximum amount of material, model B only allows region I to vaporize, and model C uses all of the energy in region I to vaporize material in region I and the energy in region II to vaporize as much material as possible in region II.

A series of calculations of the amounts of vaporized mass has been carried out with CONRAD for target yields ranging from 3.0 MJ to 450 MJ, the results of which are presented in Fig. 6. One can see that the vaporized mass can vary by a factor of several between the results of models B and C. This difference is due in part to the long tail on the deposition profile seen in Fig. 4. Calculations were not done for model A, which is considered to be the least physically correct of the three, and is rarely used.

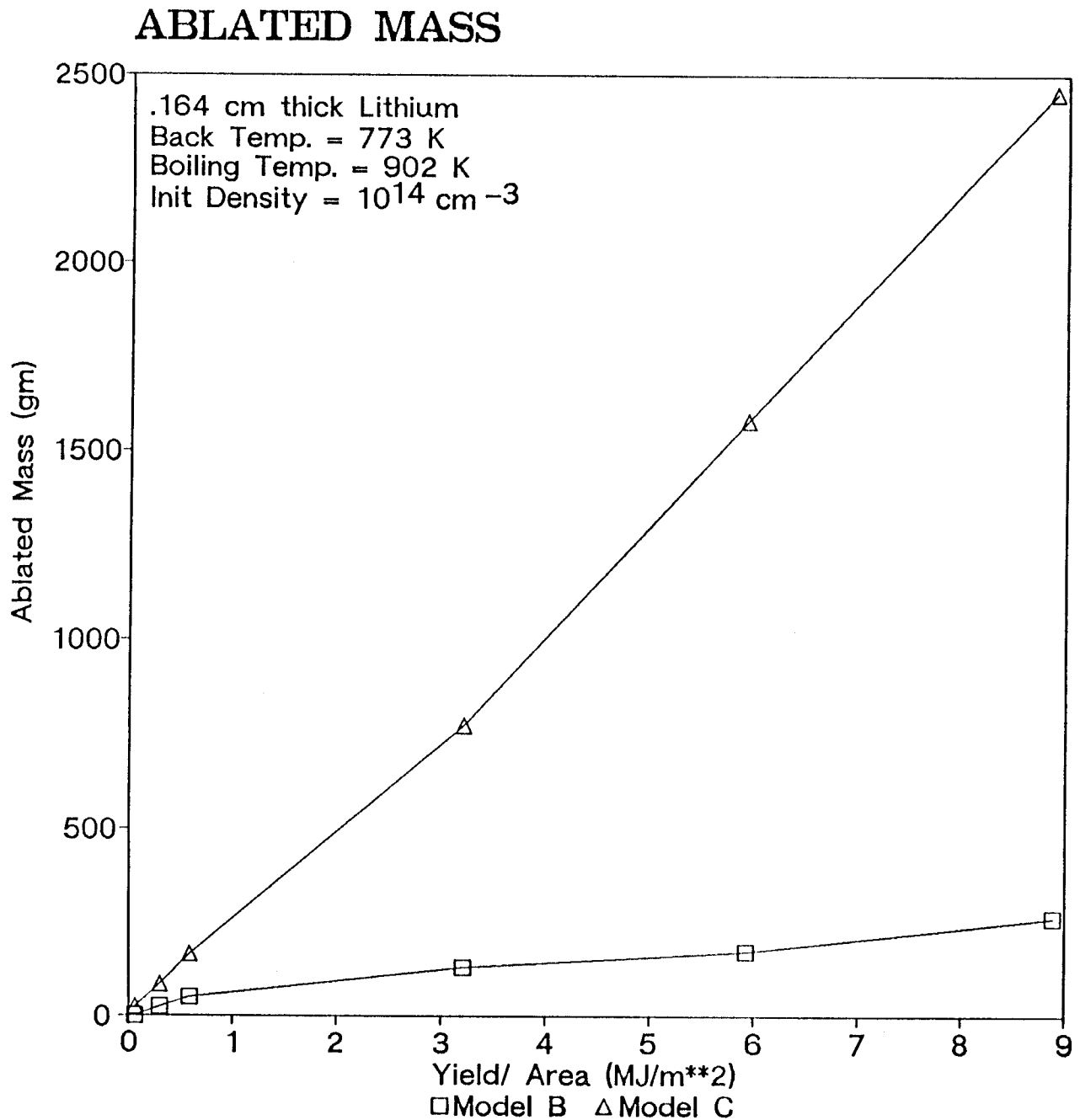
VI. CONDENSATION OF VAPORIZED MATERIAL

Condensation calculations have been carried out for three target chamber designs with the CONRAD computer code, with the microscopic evaporation model invoked. The three all allow partial vaporization of the first walls by target generated x-rays. Typical parameters for the three designs are listed in Table III. The parameters listed in this table have been fixed for the sake of example and tend to change in time as work continues on these concepts. For this reason, it is unfair to criticize these target chamber concepts on the basis of the results presented here. HIBALL uses a coating of liquid lithium-lead eutectic, $\text{Pb}_{83}\text{Li}_{17}$, on a substrate of silicon-carbide fabric to protect the rest of the structure from the target generated x-rays

Table III. Parameters for Three Target Chamber Designs

	<u>HIBALL</u>	<u>Wetted-Wall</u>	<u>CASCADE</u>
First Wall Material	Liquid Pb-Li	Liquid Li	Graphite
Target Yield (MJ)	396	25	334
Target Design	"Bangerter"	"Bangerter"	"Bangerter"
Fraction of Yield in X-rays and Ions	0.27	0.27	0.27
Distance from Target to First Wall (m)	5	2	3
X-Ray and Ion Energy per Unit Area (MJ/m ²)	0.340	0.134	0.797
Desired Rep Rate per Cavity (Hz)	5	10	5

Fig. 6. Vaporized Masses for a Two Meter Radius Spherical Target Chamber With a Liquid Lithium First Surface Versus Target Yield per Unit Target Chamber Surface. Calculations have been made within model B and C.



and ions. The chamber radius is 5 m and the hoped for repetition rate is 5 Hz. The wetted-wall concept uses liquid lithium that is rapidly flowing so that centrifugal force holds it up against a metal wall. The radius is only 2 m but the target yield is only 25 MJ, compared with 396 MJ for HIBALL. The designers of wetted-wall target chambers hope to run at 10 Hz. CASCADE is not a spherical design but has an effective radius of 3 meters and a first wall made of flowing graphite pellets that are also held against the walls by centrifugal force. Some versions of the CASCADE design use beryllium-oxide in place of graphite, but it has since been learned that BeO will dissociate and the beryllium will condense, leaving a great deal of oxygen gas in the the cavity that must be pumped out.⁸ The target yield is 334 MJ. As one can see from Table III, the x-ray and ion target energy per unit area varies considerably between the three designs and the designs have different wall materials. The average gas densities in the HIBALL, the wetted-wall concept, and CASCADE target chambers, as simulated by CONRAD, are shown in Figs. 7, 8, and 9 respectively. In all of these calculations, the target chambers are treated as being spherical.

The results for HIBALL show that after 0.2 seconds the density is still $5 \times 10^{14} \text{ cm}^{-3}$, more than 2 orders of magnitude higher than that required for ballistic focusing. This is because the thermal speed of the vapor atoms is very low because most of the energy has been radiated away and the high mass of the lead atoms. One should notice the vapor density is actually increasing very early in the calculation, which is due to the high radiant heat flux. The vapor density in the wetted-wall concept initially falls very rapidly to below 10^{14} cm^{-3} but then condensation ceases. At this point the evaporation rate is equal to the condensation rate. The evaporation rate is fairly high

Fig. 7. Average Vapor Density in HIBALL Target Chamber Versus Time.

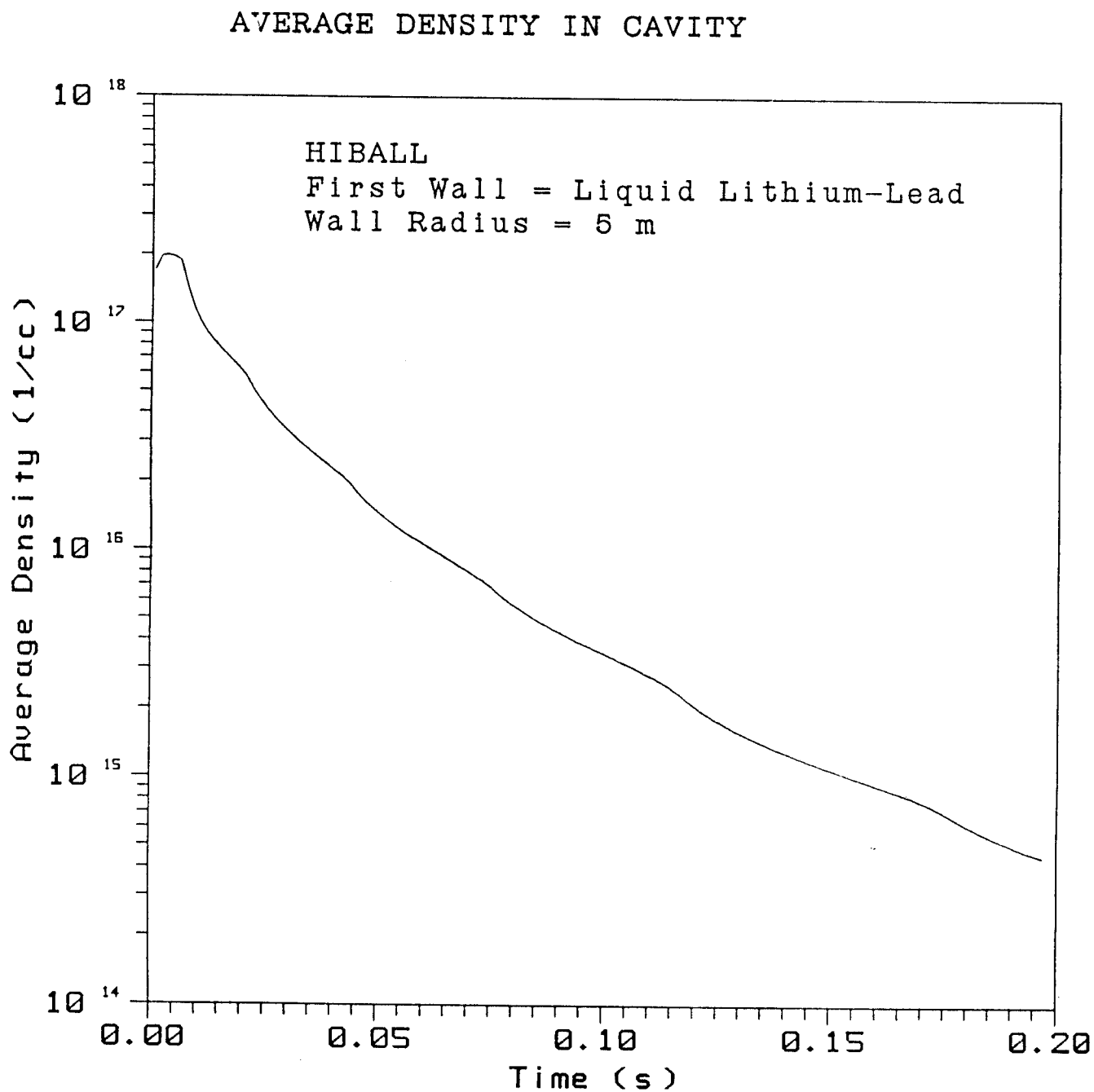


Fig. 8. Average Vapor Density in a Wetted-Wall Target Chamber Versus Time.

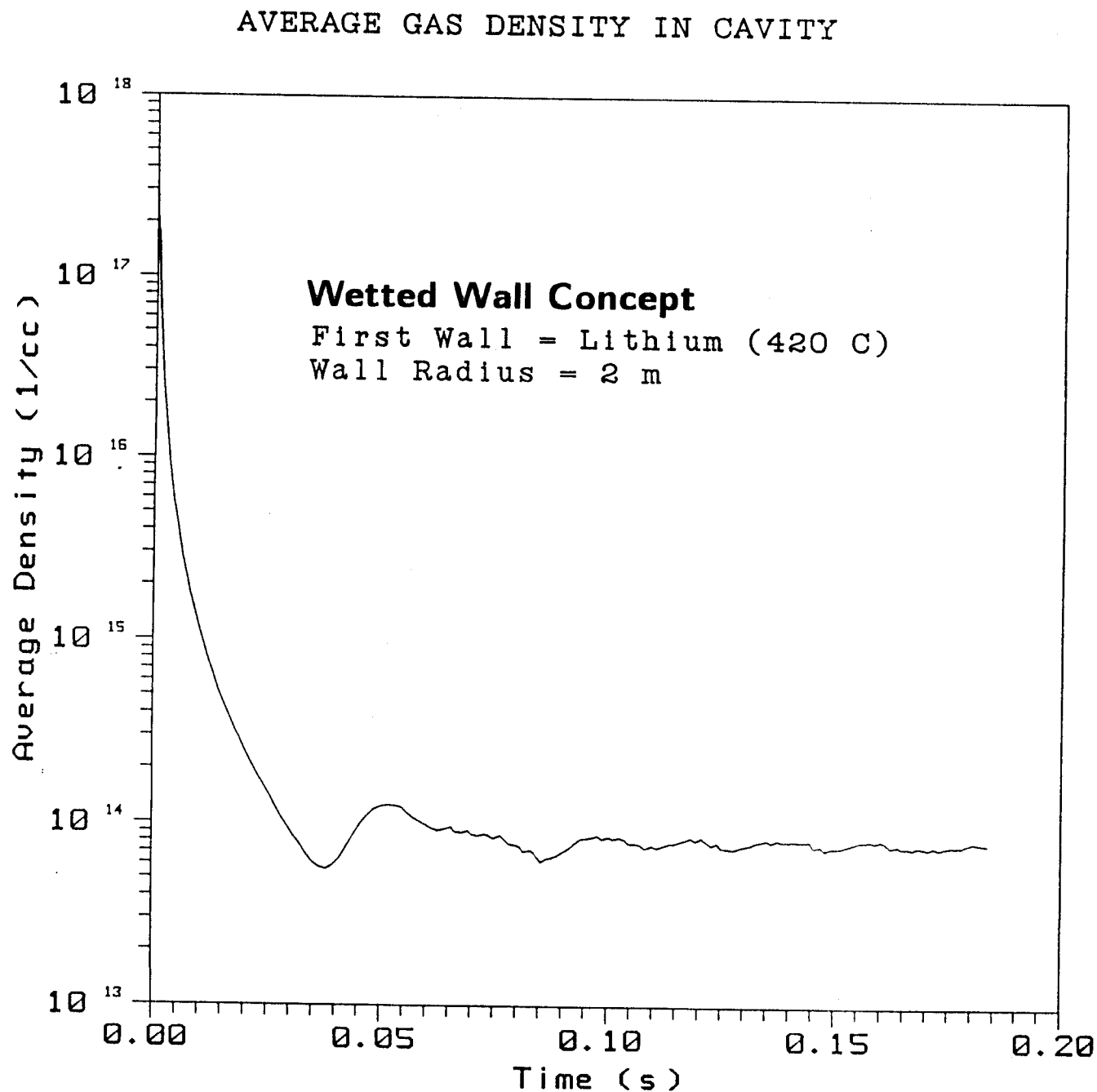
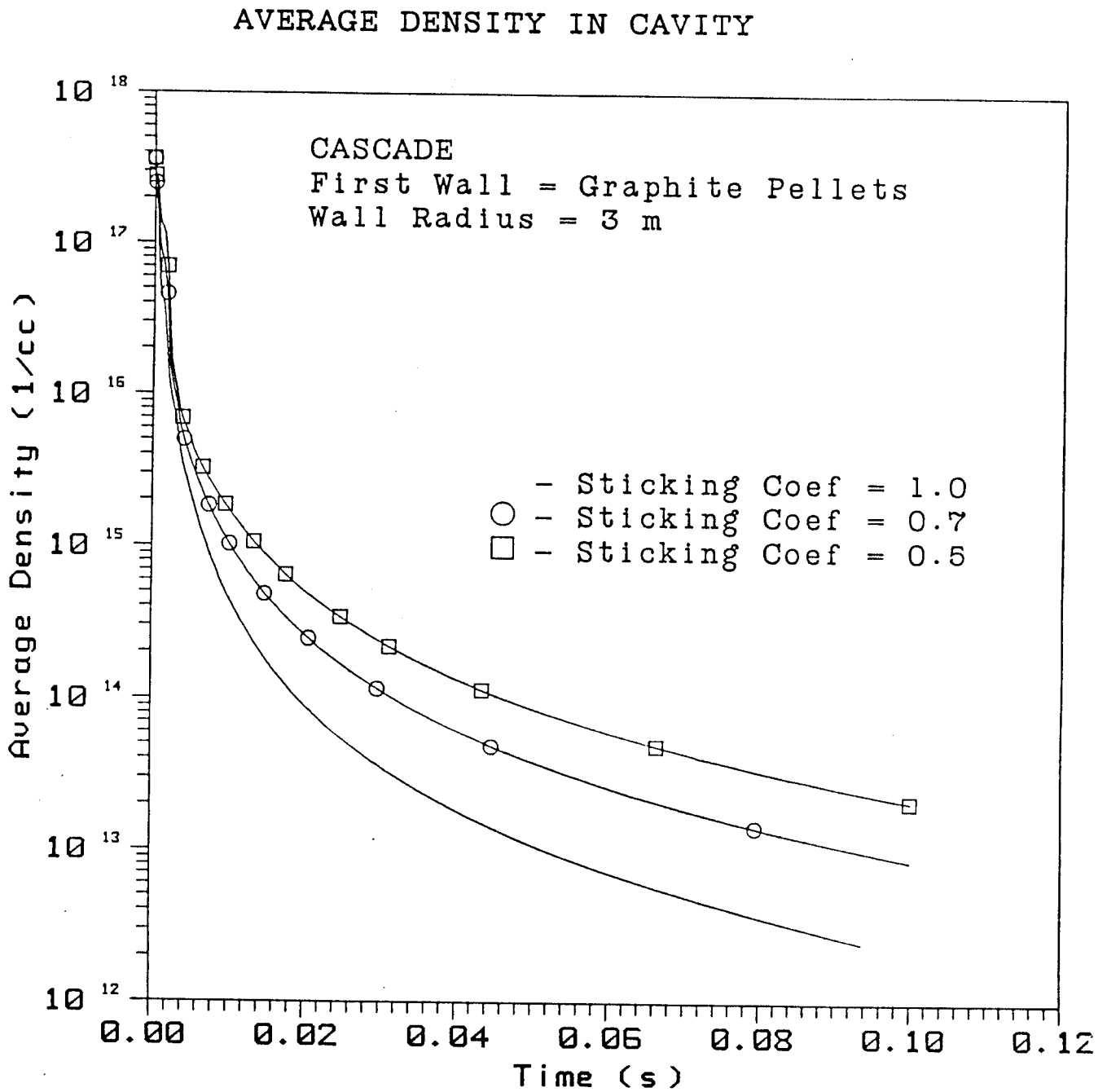


Fig. 9. Average Vapor Density in CASCADE Target Chamber Versus Time.



because the temperature of the surface of the liquid lithium is 540°C at 0.1 second. The condensation could continue if the bulk temperature of the liquid lithium were lowered below 420°C or if some other way of increasing the heat transfer could be found. The thermal conductivity has already been increased over classical values in an attempt to account for convective heat transfer. A set of three calculations has been done for CASCADE, for three values of the sticking coefficient for vapor atoms striking the surface. If all of the atoms striking the surface stick to it, a sticking coefficient of 1, the density of vapor in the cavity falls to the level required for ballistic focusing, $3 \times 10^{12} \text{ cm}^{-3}$, in less than 0.1 second. It has been found, however, that because of the chemistry of vaporized carbon the sticking coefficient may be about 0.7.¹⁰ This leads to a density of $1 \times 10^{13} \text{ cm}^{-3}$ at 0.1 second and should lead to a level acceptable for ballistic focusing by 0.2 second. If the correct value is actually 0.5, condensation occurs too slowly to allow a 5 Hz repetition rate and ballistic focusing.

There has been some indication that ballistic focusing may indeed be possible at densities of more than 10^{14} cm^{-3} .²² If this is true, there is no problem for the wetted-wall concept and CASCADE in running at 10 Hz. HIBALL may marginally be able to run at 5 Hz.

VII. ALLOWABLE REPETITION RATES

Computer simulations of the condensation of target explosion created vapor in three designs of HIF target chambers have been carried out. If the relatively hard vacuum of $3 \times 10^{12} \text{ cm}^{-3}$ is required for ballistic ion beam focusing, one has three different concerns for the three designs, each of which could make the repetition rate unacceptably high. In the case of

HIBALL, the vapor can cool rapidly due to radiation so that the thermal speed can become very low and the cavity is so large that it takes too long for the vapor atoms to reach the surface. In the wetted-wall concept, the vapor pressure of the liquid lithium is high at fairly low temperatures so that the condensation can be greatly slowed if the surface temperature of the lithium is even as high as 540°C. In CASCADE, the chemistry of the vapor causes the sticking coefficient of the vapor on the surface to be significantly below 1.

Adjustments to the parameters listed in Table III may improve the repetition rates. In HIBALL, the rate may be increased by making the cavity smaller, and in the wetted-wall concept increasing the flow rate of the lithium may lower the vapor pressure by lowering the bulk temperature of the lithium and increasing convective heat transfer. It is harder to say what can be done to CASCADE to change the chemistry of the vapor, but the search for improvement must begin by gaining understanding of the physics of such hot and dense vapors. If it is indeed possible to focus the ion beams through denser gases, all three designs show promise of allowing reasonable repetition rates.

VIII. CONCLUSIONS

Vaporization and condensation phenomena in HIF target chambers can be critically important in determining the repetition rate of the facility. These phenomena are most important to designs that require very low target chamber gas densities at the time of driver beam propagation, such as designs requiring ballistic beam focusing. The density required varies by six orders of magnitude, depending on the propagation mode.

There are several physics issues that are important to understanding vaporization and condensation phenomena. Heat transfer through the vaporizing

or condensing surface is clearly important when the thermal diffusion time is comparable to or shorter than the time over which heat is deposited. The conditions of the vapor, that is its temperature and density, can have a large effect on the condensation of the gas. The physics of sticking, which may be greatly influenced by the chemistry of the vapor phase, can also dominate the condensation rate.

A computer code is under development that simulates these phenomena in ICF reactor target chambers. Presently, the CONRAD code models vaporization, hydromotion and ionization in the vapor, radiative heat transfer from the vapor back onto the surface, and condensation. The detailed physics of sticking and vapor chemistry are not presently included in the code. To date, CONRAD has been used to show the importance of radiative heat transfer, of correct modeling of the vaporization process, of using the proper target x-ray spectrum, of calculating the heat transfer in the surface, and of properly modeling the evaporation of material during the condensation phase.

Experimentation is needed to benchmark computer codes and study specific physics issues. Many of the physics issues rely on models that need experimental verification. For example, there are presently at least three candidate models for vaporization, where each gives a different result. Experiments are needed to better understand the details of this complicated process. Even if all of the individual physics issues are understood, experiments that involve all of the issues together are needed to test the validity of the computer codes such as CONRAD.

The CONRAD computer code is being subjected to a verification procedure through comparison with some experimental data. This process has already lead to improvements in the manner ions are absorbed in the gas and will doubtless

lead to more improvements. Once this process has been completed and a better version of CONRAD is available, we will be able to study HIF target chamber phenomena more completely than we can at the present time. One area to which we expect to devote considerable effort is the interaction of the target ions with newly created vapor and the subsequent behavior of the vapor shortly after the target explosion.

ACKNOWLEDGMENT

Parts of this work have been supported by Los Alamos National Laboratory, Lawrence Livermore National Laboratory, U.S. DOE, and Kerforschungszentrum Karlsruhe. Some of the computer calculations presented here were performed at the San Diego Super Computer Center, which is supported by the National Science Foundation.

REFERENCES

1. D.S. ZUCKERMAN et al., "Performance and Cost Modelling of a LINAC-Driven HIF Power Plant," Heavy Ion Fusion, Washington, DC, 1986, AIP Conference Proceedings 152, editors M. Reiser, T. Godlove and R. Bangerter.
2. W. MEIER, W. HOGAN and R. BANGERTER, "Economic Studies for Heavy-Ion-Fusion Electrical Power Plants," Heavy Ion Fusion, Washington, DC, 1986, AIP Conference Proceedings 152, editors M. Reiser, T. Godlove and R. Bangerter.
3. R.W. CONN et al., "SOLASE - A Conceptual Laser Fusion Reactor Design," University of Wisconsin Fusion Technology Institute Report UWFDM-220 (Dec. 1977).
4. E.W. SUCOV, "Inertial Confinement Fusion Central Station Electrical Power Generating Plant," Westinghouse Fusion Power Systems Department Report WFPS-TME-81-001 (Feb. 1981).
5. B. BADGER et al., "Preliminary Conceptual Design of SIRIUS, A Symmetric Illumination, Direct Drive Laser Fusion Reactor," University of Wisconsin Fusion Technology Institute Report UWFDM-568 (March 1984).
6. B. BADGER et al., "HIBALL - A Conceptual Heavy Ion Beam Driven Fusion Reactor Study," Kernforschungszentrum Karlsruhe Report KfK-3202 and University of Wisconsin Fusion Technology Institute Report UWFDM-450 (Dec. 1981).
7. J.H. PENDERGRASS, T.G. FRANK, and I.O. BOHACHEVSKY, "A Modified Wetted-Wall Inertial Fusion Reactor Concept," Proc. 4th ANS Topl. Mtg. Technology of Controlled Nuclear Fusion, King of Prussia, Pennsylvania, October 14-17, 1980 CONF-801011, Vol. 11, P. 1131, U.S. Department of Energy (July 1981).
8. J.H. PITTS, "CASCADE: A High-Efficiency ICF Power Reactor," Lawrence Livermore National Laboratory Report UCRL-93554 (Oct. 1985).

9. R.R. PETERSON, "Gas Condensation Phenomena in Inertial Confinement Fusion Reaction Chambers," University of Wisconsin Fusion Technology Institute Report UWFDM-654 (Oct. 1985) (presented at the 1985 International Symposium on Laser Interaction with Plasma, October 1985, Monterey, CA).
10. A.J.C. LADD, "Condensation of Ablated First-Wall Materials in the CASCADE Inertial Confinement Fusion Reactor," Lawrence Livermore National Laboratory Report UCRL-53697 (Dec. 1981).
11. E. PANARELLA, "Theory of Laser-Induced Gas Ionization," Foundations of Physics, 4 (No. 2), 227-259 (1974).
12. J.F. READY, Effects of High Power Laser Radiation, Academic Press, New York (1971).
13. Ya.B. ZEL'DOVICH and Yu.P. RAIZER, Physics of Shock Waves and High-Temperature Hydrodynamic Phenomena, Academic Press, New York (1967).
14. R.E. PALMER, J.P. ANTHES, M.A. PALMER, "Effect of Background on the Propagation of a High-Intensity Laser Beam to a Target," Technical Digest of the Topical Meeting on Inertial Confinement Fusion, February 26-28, 1980, San Diego, CA.
15. P.A. MILLER et al., "Propagation of Pinched Electron Beams for Pellet Fusion," Phys. Rev. Lett., 39, 92 (1977).
16. G. COOPERSTEIN et al., "NRL Light Ion Beam Research for Inertial Confinement Fusion," Naval Research Laboratory Memorandum Report 4387 (November 1980).
17. J.R. FREEMAN, L. BAKER and D.L. COOK, "Plasma Channels for Intense-Light-Ion-Beam Reactors," Nucl. Fusion, 22, 383 (1982).
18. J.N. OLSEN and R.J. LEEPER, "Ion Beam Transport in Laser Initiated Discharge Channels," J. Appl. Phys., 53, 3397 (1982).

19. R.R. PETERSON, G.A. MOSES and G.W. COOPER, "Cavity Gas Analysis for Light Ion Fusion Reactors," Nucl. Tech./Fusion, 1, 377 (1981).
20. Z.G.T. GUIRAGOSSIAN, "Description of a Novel Light Ion Accelerator System for ICF," Bull. Am. Phys. Soc., 24, 1033 (1979).
21. C.L. OLSON, "Ion Beam Propagation and Focusing," J. Fusion Energy, 1, 309 (1981).
22. P. STROUD, "Streaming Modes in HIF Beam Final Transport," Los Alamos Report LA-UR-85-2809 (1985).
23. B. BADGER et al., "HIBALL - A Conceptual Heavy Ion Beam Driven Fusion Reactor Study," Kernforschungszentrum Karlsruhe Report KfK-3202 and University of Wisconsin Fusion Technology Institute Report UWFD-450 (1981) pp. V.6-1 to V.6-5.
24. R.R. PETERSON and T.J. BARTEL, "ICF Reactor Target Chamber Issues for the Los Alamos National Laboratory FIRST STEP Reactor Concept," University of Wisconsin Fusion Technology Institute Report UWFD-580 (1984).
25. R.R. PETERSON, "Liquid Metal Vaporization and Recondensation and the Repetition Rate of a Liquid Lithium First Surface Inertial Confinement Fusion Reactor," The 1984 IEEE International Conference on Plasma Science, May 1984.
26. M. MARTINEZ-SANCHEZ, MIT, private communication.
27. J. PENDERGRASS, Los Alamos National Laboratory, private communication.
28. R.R. PETERSON, "CONRAD - A Combined Hydrodynamics-Vaporization/Condensation Computer Code," University of Wisconsin Fusion Technology Institute Report UWFD-670 (April 1986).

29. Lawrence Livermore National Laboratory (LLNL) is presently providing funds to the University of Wisconsin (UW) to compare results from CONRAD with experimental data and results from other computer codes. LLNL and UW are also working on the design of experiments that could be used to verify the x-ray vaporization and condensation aspects of CONRAD.

30. B.H. RIPIN et al., "Transition Coupling Regime of Two High-Speed Interstreaming Plasmas," Bull. Am. Phys. Soc., 31, 1528 (1986) paper 6E1.

31. D.L. HANSON and M.K. MATZEN, "Comparative Study of X-Ray and Ion Beam Energy Deposition in Aluminum Using Pulsed Power Sources," Bull. Am. Phys. Soc., 30, 1504 (1985) paper 5R24.

32. J. ASMUS, N. LOTER, K. WARE and R. WILSON, "Stress and Impulse Produced by the Deposition of PRS Radiation," Bull. Am. Phys. Soc., 31, 1596 (1986) paper 8R8.

33. W.E. MAHER, "Preliminary Evaluation of Plasma Formation in Target Vapors by FEL Beam," Bull. Am. Phys. Soc., 31, 1570 (1986) paper 7R28.

34. R.R. PETERSON and G.A. MOSES, "MIXERG - An Equation of State and Opacity Computer Code," Computer Physics Communications, 28, 405 (1983).

35. "T-4 Handbook of Material Properties Data Bases," K.S. Holian, ed., Los Alamos National Laboratory Report LA-10160-MS (November, 1984).

36. T. MEHLHORN, J.M. PEEK, E.J. MCGUIRE, J.N. OLSEN and F.C. YOUNG, "Current Status of Calculations and Measurement of Ion Stopping in ICF Plasmas," Sandia Report SAND83-1519 (December 1983).

37. R.O. BANGERTER and D. MEEKER, "Ion Beam Inertial Fusion Target Designs," Lawrence Livermore National Laboratory Report UCRL-78474 (1976).

38. J.D. LINDL and J.W-K MARK, "Recent Livermore Estimates of Cryogenic Single-Shell Ion Beam Targets," Lawrence Livermore National Laboratory Report UCRL 90241 (Feb. 22, 1984).

39. G.A. MOSES, G.R. MAGELSEN, R. ISRAEL, T. SPINDLER, "PHD-IV, A Plasma Hydrodynamics, Thermonuclear Burn, Radiative Transfer Computer Code," University of Wisconsin Fusion Technology Institute Report UWFD-194 (revised January 1982).

40. G.A. MOSES, R.R. PETERSON, M.E. SAWAN and W.F. VOGELSONG, "High Gain Target Spectra and Energy Partitioning for Ion Beam Fusion Reactor Design Studies," University of Wisconsin Fusion Technology Institute Report UWFD-396 (Nov. 1980).

41. G.A. MOSES, "Frequency Dependent X-ray Fluences from a High Yield Light Ion Beam Fusion Target Explosion in a Gas Filled Chamber," University of Wisconsin Fusion Technology Institute Report UWFD-486 (September 1982).